CONSTITUTIVE RELATIONS OF MILD STEEL AND [MATH]-TITANIUM AT HIGH RATES UNDER MULTIAXIAL LOADING CONDITION

K. Mimura, Y. Tomita

JOURNAL DE PHYSIQUE IV C3-813
Colloque C3, suppl. au Journal de Physique III, Vol. 1, octobre 1991

CONSTITUTIVE RELATIONS OF MILD STEEL AND α-TITANIUM AT HIGH RATES UNDER MULTIAXIAL LOADING CONDITION

K. MIMURA and Y. TOMITA

Department of Mechanical Engineering, Faculty of Engineering, Kobe University, 1-1 Rokkodai Nada Kobe 657, Japan

Résumé : Cet article apporte une contribution à la connaissance du critère de plasticité en situation de chargement multiaxial dynamique. On obtient expérimentalement les relations contrainte -déformation pour le S25C et l'alpha-titane associées à un trajet de chargement linéaire ou bilinéaire à différentes vitesses de défomation. On peut ainsi tracer dans l'espace "contrainte axiale - contrainte de cisaillement - déformation plastique totale" les surfaces d'équi-déformation. De plus, afin de décrire l'évolution de ces surfaces, un modèle d'écrouissage cinématique rattaché au modèle de Perzyna a été introduit. Dans ce modèle, l'évolution du centre du critère de plasticité dépend de l'amplitude du dépassement du critère et de l'histoire du chargement. Les simulations fondées sur ce modèle font apparaitre des surfaces d'équi-déformation en bon accord avec les résultats obtenus avec l'alpha-titane. Cependant, pour le S25C, on note certaines différences entre les prédictions numériques et le résultat expérimental.

ABSTRACT This paper provides some prospect of comprehension of the dynamic yield criterion under multiaxial loading. The stress - strain relations for S25C and α-titanium along linear or bilinear strain paths at several strain rates were measured experimentally, and the obtained equi-plastic strain surfaces of both metals were plotted within axial-torsional stress plane. Further more in order to describe the behavior of these equi-plastic strain surfaces, kinematic hardening model in conjunction with the Perzyna type overstress was introduced. In this model, the evolution of a center of a yield surface is affected by the magnitude of overstress and loading histories. The simulation of equi-plastic strain surfaces based on the proposed model well expresses the results of α-titanium. However, for S25C there are some difference between the numerical prediction and the experimental results.

1. INTRODUCTION

Over recent years numerous experimental investigations have been made to establish constitutive equations which describe the mechanical behavior of materials under dynamic loading. However, in many cases they employed the uniaxial loading condition and there are a few reference to multiaxial stress states [1-3]. On the other hand in the practical use, since materials are subjected to the multiaxial loads, and strain rate or loading direction is frequently changed, it is of increasing importance to verify whether constitutive relationship such as strain rate sensitivity or effect of strain rate history obtained from the results of uniaxial loading tests, retain its validity under multiaxial loading condition. Whereas in this field, only limited data are available.

In the present paper, in order to clarify the influence of strain rate and strain rate history on initial and subsequent yield criteria under multiaxial loading, two kinds of biaxial loading tests were carried out on S25C and α-titanium in the strain rate range from 10^{-5}/s to 10^{4}/s. One is the proportional loading (=linear loading) test with a constant strain rate to examine the initial anisotropy and the rate sensitivity of a material. The other is the bilinear loading test with a change

in strain rate to investigate the effect of strain rate history on a subsequent yield condition. The latter experiment corresponds to "strain rate jump test" under multiaxial loading condition, i.e. not only a strain rate but also a loading direction is rapidly changed at a certain strain point. In this case, as discussed in the later section, we must take into account the effect of strain history as well as strain rate history when the constitutive relations are formulated.

2. EXPERIMENTAL APPARATUS AND PROCEDURE

Three kinds of testing devices were employed to perform the biaxial experiments : (1) hydraulic proof system (HPS), (2) clamp type split Hopkinson bar (CSHB) and (3) oblique plate edge-impact testing device (OPEI). Each device covers the strain rate range 10^{-4}/s~10^{1}/s, 10^{2}/s~10^{3}/s and 10^{3}/s~2×10^{4}/s, respectively. In the bilinear loading test, the first path was given quasistatically in the axial direction and the second path was given dynamically at several strain rates in various directions. The length of the first straining path is 1.5% for α-titanium and 2.0% for S25C, respectively. Since the combination of HPS and a thin-walled tubular specimen is popular for the biaxial experiment, brief explanation about the CSHB and the OPEI is given here.

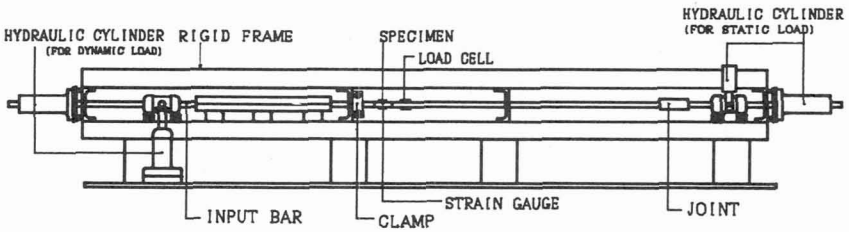

Figure 1. Clamp type Split Hopkinson Bar

Figure 1 shows the schematic drawing of the CSHB. A thin-walled tubular specimen with inner diameter of 13mm, outer diameter of 14mm and gauge length of 5mm was employed in the experiment. The axial and torsional strain on a specimen is measured directly with strain gauges. The hydraulic systems on the left hand side in the figure are used to store the elastic energy in the incident bar, while the other hydraulic systems on the right hand side are used to give a specimen quasistatic load. This mechanism gives the CSHB the ability of "strain rate jump" from quasistatic strain rate to an elevated one.

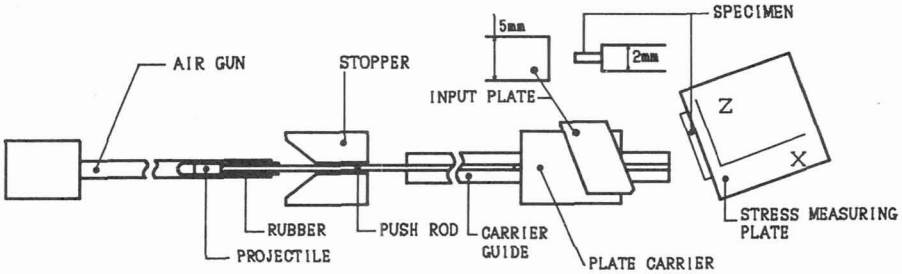

Figure 2. Oblique Plate Edge-Impact Device

Figure 2 shows the outline of the OPEI. In this device, only proportional loading is applicable. A thin rod specimen with length of 120mm, width of 2mm and thickness of 1mm was put on the edge of the stress measuring plate and obliquely impacted by the input plate. The axial strain ε_x and shear strain γ_{xz} on a specimen are measured by the strain gauges with the gauge length of 0.2mm. Here,

since the micro grooves on the edge of the input plate and the stress measuring plate prevent the deformation of a specimen in z-direction, we can assume that ε_z is almost 0.

3. CONSTITUTIVE MODELING

In this section, we consider the rate sensitive constitutive equations where the effect of strain history and strain rate history under multiaxial loading condition are taken into account. First, we suppose that materials are initially von Mises bodies. Thus, yield function f is given by :

$$f = \frac{3}{2}(S_{ij} - \alpha'_{ij})(S_{ij} - \alpha'_{ij}) - \overline{\sigma}_y^2 \qquad (1)$$

where, S_{ij} and α'_{ij} denote the deviatoric components of stress and backstress, respectively. $\overline{\sigma}_y$ is the yield radius at quasistatic strain rate and is the function of effective plastic work W^p :

$$\overline{\sigma}_y = \sigma_o(1 + R\, W^{p^n}) , \quad \dot{W}^p = [(\sigma_{ij} - \alpha_{ij})/\sigma_o]\, \dot{\varepsilon}^{vp}_{ij} \qquad (2)$$

where, n is a material constant. σ_o denotes the initial yield stress of a material. Employing Perzyna's constitutive relation [4], overstress F is defined as :

$$F = [\frac{3}{2}(S_{ij} - \alpha'_{ij})(S_{ij} - \alpha'_{ij})]^{1/2} / \overline{\sigma}_y] - 1 \qquad (3)$$

By assuming the normality rule, visco-plastic strain rate $\dot{\varepsilon}^{vp}_{ij}$ is given by :

$$\dot{\varepsilon}^{vp}_{ij} = \eta \ \langle \Phi \rangle \frac{\partial F}{\partial \sigma_{ij}} , \quad \eta = 2\, \overline{\sigma}_y \qquad (4)$$

In equation (4), $\langle \Phi \rangle$ is widely noted as the "overstress function" which prescribes the relation between visco-plastic strain rate and overstress F. With respect to Φ, various formulations have been proposed. These constitutive formulations are classified systematically in reference [5]. In the present research, the following relation proposed by Hojo and Chatani[6] is employed.

$$\Phi = \frac{K_1}{\Gamma_T + \Gamma_V} \qquad (5)$$

where, Γ_T and Γ_V denote the terms of thermal activation and viscous drag, respectively. The definition of Γ_T and Γ_V is shown in Fig.3. Each term is given by :

$$\Gamma_T = \exp\{K_2 - K_3(F + K_5)\} \qquad (6.a)$$

$$\Gamma_V = \exp\{K_4/(F + K_5)\} \qquad (6.b)$$

where, $K_1 \sim K_4$ are material constants. K_5 is the newly introduced parameter so that overstress F becomes nearly 0 at the quasistatic rate, 10^{-5}/s [7]. The above mentioned constitutive relation does not involve the effect of strain rate history. Thus, we make here the brief discussion about the effect of strain rate history under the multiaxial loading condition. The relation between total stress τ and strain rate $\dot{\gamma}$

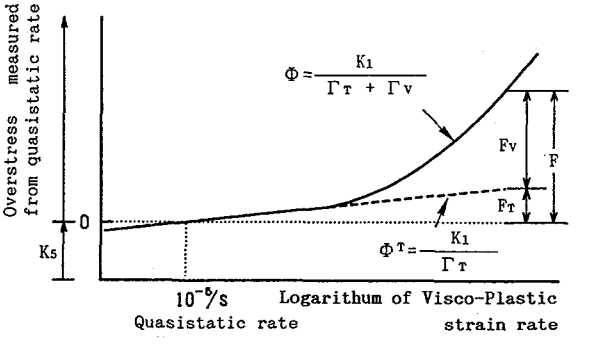

Figure 3. Definition of Overstress Function

$$\tau = A\{1+ m \ln(1+\dot{\gamma}_1/B)(\gamma)^n + \{ mA \ln[(B+\dot{\gamma}_2)/(B+\dot{\gamma}_1)]\}(\gamma-\alpha)^n$$

is widely used to express the effect of strain rate history of materials. However,

under multiaxial loading condition, the effect of strain history as well as that of strain rate history is not negligible. In general, these historical effects should be considered in the structural parameters. In this paper, we attempt to introduce the effect of strain history and strain rate history into kinematic hardening rules. First, we consider the internal structural tensor ρ_{ijkl} which memorizes the strain history[8]. The evolutional equation of ρ_{ijkl} is given by :

$$\dot{\rho}_{ijkl} = D_P \left(\frac{2}{3}E_{ij}\frac{2}{3}E_{kl} - \rho_{ijkl}\right)\dot{\bar{\varepsilon}}^{vp} \tag{7}$$

where, $\dot{\bar{\varepsilon}}^{vp}$ and E_{ij} denote equivalent visco-plastic strain rate and normalized visco-plastic strain rate, respectively. They are defined by :

$$\dot{\bar{\varepsilon}}^{vp} = \left[\frac{2}{3}\dot{\varepsilon}^{vp}_{ij}\dot{\varepsilon}^{vp}_{ij}\right]^{1/2} \quad \text{and} \quad E_{ij} = \dot{\varepsilon}^{vp}_{ij} / \dot{\bar{\varepsilon}}^{vp}$$

When a certain set of normalized strain rates (E_{ij}) is given, the corresponding components of ρ_{ijkl} become non-zero and they are saturated to some values as the deformation progresses. Note that tensor ρ_{ijkl} has the fading memory, thus, if the different set of E_{ij} is given, the current components of ρ_{ijkl} gradually vanish and the new components are developed. Using ρ_{ijkl}, we can obtain the following scalar function which represents the nonlinearity of loading path.

$$\phi = \left[\left(\rho_{ijkl}\rho_{ijkl} - \frac{2}{3}E_{ij}\rho_{ijkl}\rho_{klmn}E_{mn}\right) / \rho_{pqrs}\rho_{pqrs}\right]^h \tag{8}$$

The function ϕ takes a certain positive value if current set of E_{ij} is different from prior one. Referencing nonlinear kinematic hardening rules proposed by Chaboche[9], we formulate the modified evolutional equations of backstress, in terms of the function ϕ, as follows :

$$\dot{\alpha}'_{ij} = \Sigma \dot{\alpha}'^{(K)}_{ij} \tag{9.a}$$

and

$$\dot{\alpha}'^{(K)}_{ij} = (1 + \chi\phi) D^{(K)}\left\{\frac{2}{3}\sigma_o C^{(K)} E_{ij} - \alpha'^{(K)}_{ij}\right\}\dot{\bar{\varepsilon}}^{vp} \tag{9.b}$$

Where χ is a material constant. If Eq.(9.a) and (9.b) are used associated with Eq.(1), they can express the cross hardening effect as well as the Bauschinger effect. Here, it seems reasonable to assume that $D^{(K)}$ and $C^{(K)}$ in Eq.(9.b) are the function of overstress F to express the strain rate history. However, their formulations are strongly influenced by the target materials; for example, titanium, copper and aluminum show the positive strain rate history, while mild steel shows the negative one. Thus, explicit forms of $C^{(K)}$ and $D^{(K)}$ for each metal are given in the next section.

4. RESULTS AND DISCUSSIONS

4.1 INITIAL YIELD CONDITION AND STRAIN RATE SENSITIVITIES OF α-TITANIUM AND S25C

The initial yield loci of α-titanium and S25C at several strain rates are shown in Fig.4.a and Fig.4.b. As shown in the figures, the difference between axial and torsional equivalent stress is very small. Thus we can suppose that the initial yield condition of both metals are von Mises type. Figure 5 shows the strain rate sensitivities of α-titanium and S25C. From the results, the material constants K_1 ~ K_5 in Eq.(5) and Eq.(6) are determined and listed in Table 1.

Table 1

Material	K_1	K_2	K_3	K_4	K_5
α-Titanium :	5.0 x10^5	39.5	26.0	10.0	0.5
S25C :	4.1 x10^4	30.0	23.5	9.5	0.44

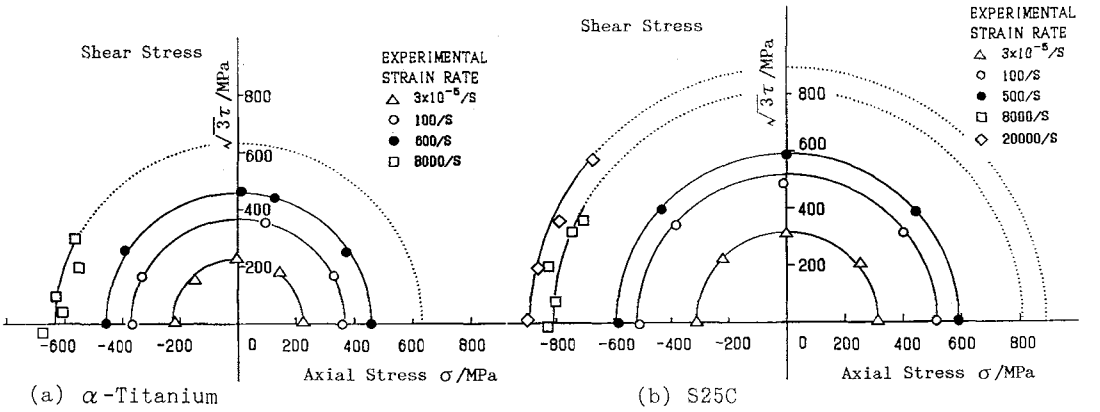

Figure 4. Initial yield loci of α-Titanium and S25C

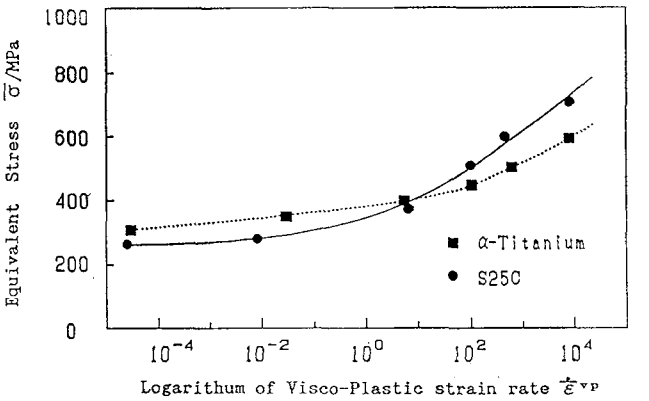

Figure 5.

Strain Rate Sensitivities of α-Titanium and S25C

4.2 STRAIN RATE HISTORY OF α-TITANIUM

Figure 6 shows the stress - strain relations for α-titanium under uniaxial loading condition. In the figures, the results of strain rate jump are also shown. In this case, the positive strain rate history effect appears and stress values following the sudden jump in strain rate gradually increase and finally coincide with those at the constant strain rates. Therefore, we can assume that $C^{(K)}$ is a material constant and only $D^{(K)}$ is the function of overstress F. Figures 7.a ~ 7.c show the results of strain rate jump under multiaxial loading condition. In the figures, experimentally obtained equi-plastic strain surfaces are expressed by broken lines. Note that strain values in the figures denote the subsequent equivalent plastic strain measured from the end of the first path. As shown in the figures, the equi-plastic strain surfaces at 600/s show the extremely rapid recovery of Bauschinger effect as compared with those at other strain rate. In the strain rate range over 600/s, the strain rate sensitivity of α-titanium is largely dependent on viscous drag, thus we define $D^{(K)}$ as a function of Fv instead of F, which is the viscous drag component of overstress as shown in Fig.3.

$$D^{(K)}=D_0^{(K)}\left(1 + \kappa_D \, Fv^m \right) \tag{10.a}$$

Equation (10.a) can be transformed into more explicit form :

$$D^{(K)} = D_0^{(K)}\left[1 + \kappa_D\left(F + K_5 - \frac{K_2 - \ln(2K_1/\dot{\bar{\varepsilon}}^{VP})}{K_3} \right)^m \right] \tag{10.b}$$

The results of numerical simulation of equi-plastic strain surface based on Eq.(1) Eq.(9) and Eq.(10) are shown in the figures by solid lines. Material constant used

in the calculation are listed in Table 2. It is found that the simulated surfaces well express the experimentally obtained equi-plastic strain surfaces.

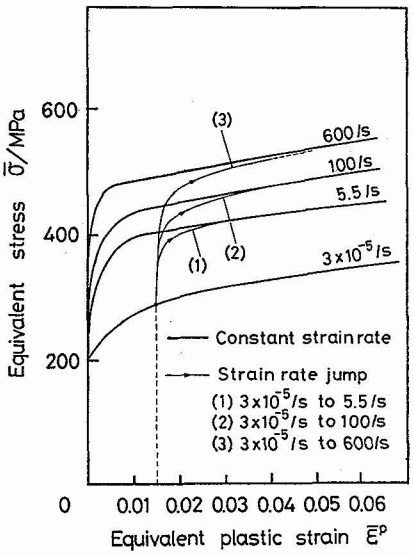

Figure 6. Stress - Strain Relation for α-Titanium

Figure 7. Equi-Plastic Strain Surface of α-Titanium

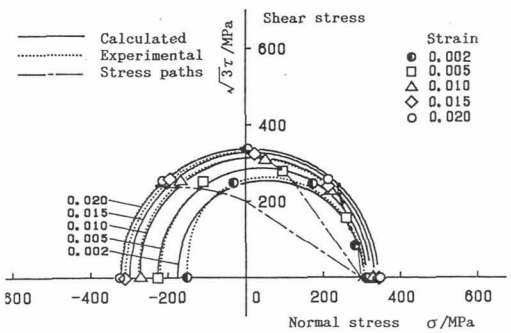

(a) Subsequent strain rate : 10^{-5}/sec

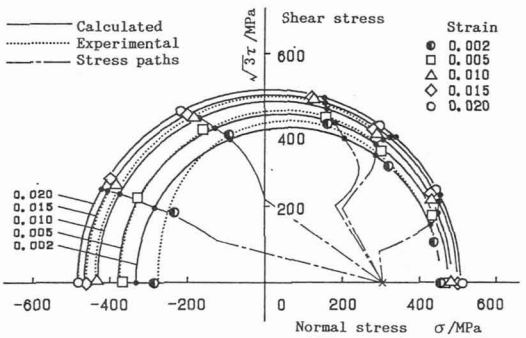

(b) Subsequent strain rate : 100/sec

Table 2

Material Constants		α-TITANIUM
* Elastic modulus	E	107GPa
* Poisson's ratio	ν	0.3
* Yield stress	σ_o	200MPa
* Isotropic hardening	R	1.0
	n	0.5
* Structural tensor	D_P	25.0
	h	1.0
* Kinematic hardening	χ	0.5
	$C_o^{(1)}$, $D_o^{(1)}$	0.5, 100
	$C_o^{(2)}$, $D_o^{(2)}$	—, —
	$C_o^{(3)}$, $D_o^{(3)}$	—, —
* Strain rate history	κ_C , κ_D	0.0, 1400
	m	2.6

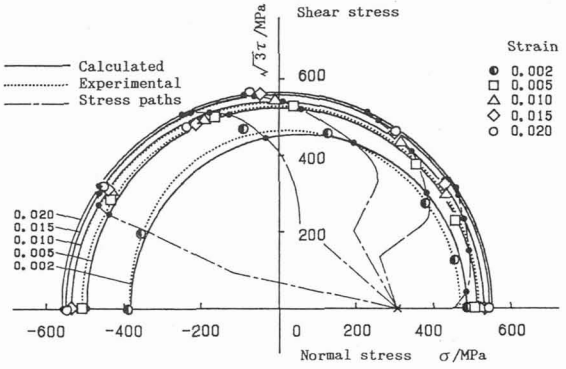

(c) Subsequent strain rate : 600/sec

4.3 STRAIN RATE HISTORY OF S25C

Figure 8 shows the stress - strain relations for S25C under uniaxial loading condition. In the case of S25C, the remarkable negative strain rate history effect appears. Stress values following the sudden jump in strain rate are considerably high as compared with those at a constant strain rate. This offset from the stress - strain curve at a constant strain rate does not decrease when the subsequent plastic strain becomes large. Furthermore, the work hardening rate at a constant strain rate becomes smaller as the applied strain rate gets higher. These facts imply that $D^{(K)}$ is a material constant but $C^{(K)}$ is getting smaller with increasing strain rate. On the other hand, it is also found that the work hardening rate following the jump in strain rate is more close to that at quasistatic rate. Thus, we suppose that $C^{(K)}$ is given by :

For constant strain rate : $$C^{(K)}=Co^{(K)}\exp(-\kappa_c F) \tag{11}$$

For strain rate jump : $$C^{(K)}= Co^{(K)}\exp(-\kappa_c F) + \bar{\alpha}^{*(K)}\{1-\exp[-\kappa_c (F-F^*)\}$$

where, $\bar{\alpha}^{(K)}$ is the norm of $\alpha^{(K)}{}_{ij}$ and superscript asterisk denotes the quantity just before the strain rate jump. Simulated stress - strain relations based on Eq.(11) are shown in the figure by solid lines. Material constants used are listed in Table 3. Simulated results show the good approximation for experimental results. However, as shown in Fig.9, under multiaxial loading condition there are significant differences between theoretical predictions and the experimental results i.e. Simulated stress on the opposite side of preloading considerably overestimated. This results show the difficulties in determination of overstress F under multiaxial loading condition.

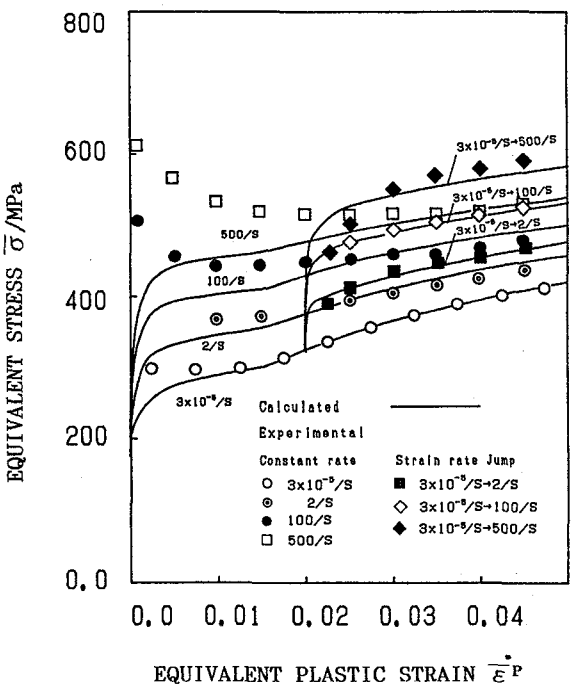

Figure 8.
Stress - strain relation for S25C

Table 3

Material Constants		S25C
* Elastic modulus	E	206GPa
* Poisson's ratio	ν	0.3
* Yield stress	σ_o	206MPa
* Isotropic hardening	R	——
	n	——
* Structural tensor	D_P	35.0
	h	0.6
* Kinematic hardening	χ	0.4
	$Co^{(1)}$, $Do^{(1)}$	0.65, 26
	$Co^{(2)}$, $Do^{(2)}$	0.50, 800
	$Co^{(3)}$, $Do^{(3)}$	0.65, 26
* Strain rate history	κ_C , κ_D	0.35, 0.0
* Notation	For S25C $Co^{(3)}$,$Do^{(3)}$ are defined $\bar{\varepsilon}^{vp} > 0.015$	

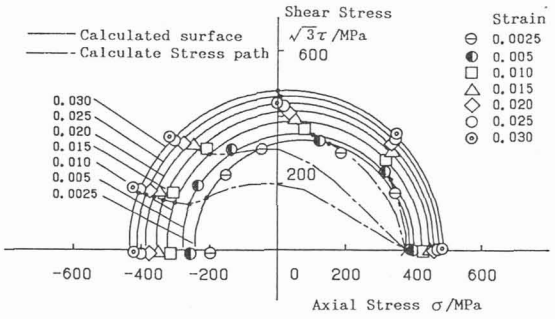

(a) Subsequent strain rate : 10^{-5}/sec

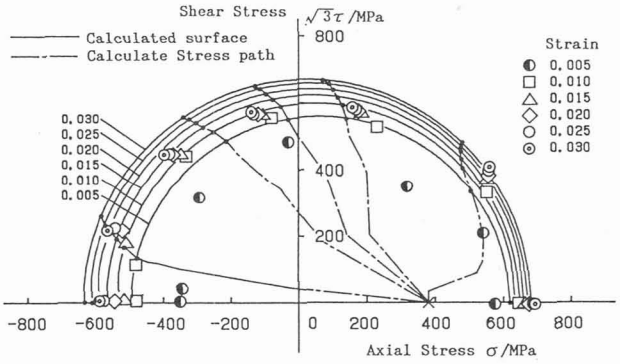

(b) Subsequent strain rate : 500/sec

Figure 9. Equi-Plastic Strain Surface of S25C

5. CONCLUSIONS

The strain rate jump tests under the multiaxial loading condition were carried out on α-titanium and S25C in order to investigate the influence of strain history and strain rate history on subsequent loading. The obtained equi-plastic strain surfaces at high strain rate are not the simple expansion of the corresponding quasistatic surfaces. In the case of α-titanium, the theoretical predictions show the good agreement with the experimental results. However, in the case of S25C, there are some differences between the simulated results and experimental results.

REFERENCES

/1/ Hojo,A. and Chatani,A., Bulletin of JSME 22(1979)469
/2/ Stiebler,K., Kunze,H.D. and Staskewitsch,E., Mechanical Properties of Materials at High Rate of Strain (1989)181, Inst. of Phys. Conf. Ser.102
/3/ Shindo,A.,Sato,M. and Mimura,K., Proc. of Impact Loading and Dynamic Behavior of Materials (IMPACT 87) 2(1988)565
/4/ Perzyna,P., Q. Appl. Math. 20(1963)321
/5/ Harding,J., Mechanical Properties of Materials at High Rate of Strain (1989)189 Inst. of Physics Conf. Ser.102
/6/ Hojo,A. and Chatani,A., J. of Soc. of Mat. Sci. Japan, 34-387(1985)1400
/7/ Mimura,K. and Shindo,A.,Proc. of Advanced Technology of Plasticity 3(1990)1587
/8/ Shindo,A., Mimura,K. Proc. of Advances in Plasticity 1989, (1989)107
/9/ Chaboche,J.L. and Rousselier,G. Trans. of ASME, 105(1983)153